

# Organically Modified Layered Silicates as Reinforcing Fillers for Natural Rubber

S. Joly, G. Garnaud, R. Ollitrault, and L. Bokobza\*

Laboratoire PCSM, E.S.P.C.I., 10 rue Vauquelin, 75231 Paris Cedex, France

J. E. Mark

Department of Chemistry and the Polymer Research Center, The University of Cincinnati, Cincinnati, Ohio 45221-0172

Received February 26, 2002. Revised Manuscript Received June 14, 2002

Rubber compounds based on natural rubber containing organically modified montmorillonites were prepared. The state of dispersion of the clay was characterized by scanning and transmission electron microscopies, and the spacings between the silicate layers were evaluated by X-ray diffraction. The effect of the addition of clay on the elastomeric compound was analyzed through mechanical and swelling properties and also through the determination of polymer chain orientation during elongation.

## Introduction

Addition of an inorganic component to polymers leads to improvements in various physical and mechanical properties. These improvements are the result of a complex interplay between the properties of the individual constituent phases: the polymer, the filler, and the interfacial region. Filler morphology such as the particle size, structure, and aspect ratio (length/diameter) have a large influence on the physical performance of the polymer composite.

Phyllosilicates have attracted a great deal of interest owing to their intrinsically anisotropic characters and swelling capabilities. Among these materials, montmorillonite is probably the most studied in both academia and industry. The crystal structure of a layered silicate such as montmorillonite consists of two-dimensional layers obtained by combining two tetrahedral silica layers with Mg or Al to form an octahedral metal oxide structure. Each layer (about 1-nm thick) is separated from the next by an interlayer or a gallery containing cations ( $\text{Na}^+$ ,  $\text{K}^+$ ,  $\text{Ca}^{2+}$ ...) which balance the excess negative charge created by a natural substitution of some atoms forming the crystal. A primary particle is composed of many silicate layers. The interlayer cations are usually replaced by alkylammonium, phosphonium, or sulfonium cations to make the normally organophilic silicate more compatible with a typical organic matrix. These bulky cations also increase the interlayer distance to an extent that is easily measurable. If energetically favorable interactions exist between the modified silicate and the polymer, then the polymer chains can be inserted between the silicate layers, further increasing the interlayer spacing and leading to an ordered multilayer with a repeat distance of a few nanometers. If the polymer and the silicate are not compatible, ag-

glomerates of layered silicate surrounded by polymer are formed. Thus, in the use of such clays as fillers in polymer systems, three general types of composite materials may be obtained (Figure 1): (a) conventional composites containing clay tactoids of stacked layers in a coplanar orientation associated in aggregates and agglomerates dispersed as a segregated phase, (b) intercalated nanocomposites, and (c) exfoliated nanocomposites. The best situation, with regard to polymer reinforcement, is the exfoliation limit, with a dispersion of the silicate layers in the polymer matrix. When dispersed into the host matrix at the nanoscale level (giving a very large polymer/filler interface), intercalated nanocomposites exhibit major improvements in various properties even at very low clay contents (<10 wt %), relative to conventional fillers.<sup>1–9</sup> Exfoliated clay phases further enhance the properties relative to the intercalated ones.

While organoclays have been largely used in various thermoplastics, a very small number of studies are reported on the use of organically modified layered silicates to reinforce elastomers.<sup>10,11</sup> In fact, elastomeric materials are usually reinforced with carbon black or

(1) Pinnavaia, T. J.; Lan, T.; Wang, Z.; Shi H.; Kaviratna, P. D. In *Nanotechnology. Molecularly Designed Materials*; Chow, G.-M., Goncalves, K. E., Eds.; American Chemical Society: Washington, D.C., 1996; Vol. 622, p 250.

(2) Krishnamoorti R.; Giannelis, E. P. *Macromolecules* **1997**, *30*, 4097.

(3) Vaia R. A.; Giannelis, E. P. *Macromolecules* **1997**, *30*, 7990, 8000.

(4) Tyan, H.-L.; Wei, K.-H.; Hsieh, T.-E. *J. Polym. Sci., Polym. Phys.* **2000**, *38*, 2873.

(5) Zanetti, M.; Camino, G.; Thomann, R.; Mülhaupt, R. *Polymer* **2001**, *42*, 4501.

(6) Chang, J.-H.; Park, D.-K.; Inh, K. J. *J. Polym. Sci., Polym. Phys.* **2001**, *39*, 471.

(7) Zerda, A. S.; Lesser, A. J. *J. Polym. Sci., Polym. Phys.* **2001**, *39*, 1137.

(8) Biswas, M.; Sinha Ray, S. *Adv. Polym. Sci.* **2001**, *155*, 167.

(9) Kornmann, X.; Lindberg, H.; Berglund, L. A. *Polymer* **2001**, *42*, 4493.

(10) Burnside S. D.; Giannelis, E. P. *Chem. Mater.* **1995**, *7*, 1597.

(11) van Amerongen, G. J. *Rubber Chem. Technol.* **1964**, *37*, 1065.

\* To whom correspondence should be addressed. E-mail: Liliane.Bokobza@espci.fr.

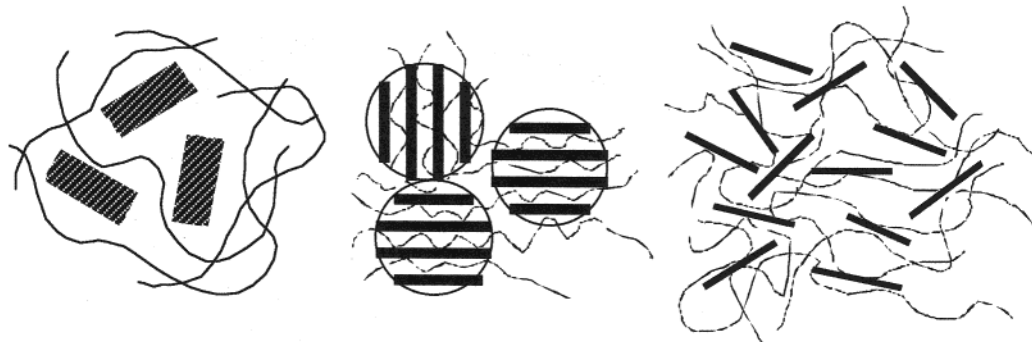


**Figure 1.** Schematic representation of the three types of polymer–clay composites.

silica, and one parameter which limits the capabilities of these fillers is their agglomeration. Direct interparticle contacts are important in a highly polar filler such as silica. Because of this, silica is usually treated to deactivate some of the reactive groups on the particle surfaces. Reducing the interactions between the particles in this way improves the dispersion of the filler in the elastomer. Silane coupling agents can also be used to help the dispersion into the elastomeric matrix and to improve filler–rubber adhesion. An alternative approach to avoid a high degree of aggregation is to precipitate silica into a network by a sol–gel technique. A typical reaction of this type involves the catalytic hydrolysis of the tetraethoxysilane. Another alternative is based on the interlayer expansion of organoclays which leads to the increased surface-to-volume ratios conducive to good filler-reinforcing capability.

This paper describes investigations carried out on natural rubber (NR) loaded with organosilicates. The morphologies of the organosilicate clays were characterized by scanning electron microscopy (SEM) and transmission electron microscopy (TEM), and the interlayer spacings were determined by small-angle X-ray scattering (SAXS). In addition to mechanical and swelling measurements, Fourier transform infrared dichroism and birefringence were used to analyze the orientational properties of the various elastomeric networks.

## Experimental Section

**Materials.** Very recently, several groups have studied composites based on *cis*-1,4-polyisoprene, natural rubber, and epoxidized natural rubber, and organically modified montmorillonite.<sup>12–14</sup> The organically modified clays used in one of these studies were bis(2-hydroxyethyl) methyl tallow ammonium montmorillonite (M1), dimethyl dihydrogenated-tallow ammonium montmorillonite (M2), and dimethyl hydrogenated tallow (2-ethylhexyl) ammonium montmorillonite (M3).<sup>13</sup> In the present extension of this work, the nonpolar nature of natural rubber suggested that M2 and M3 were the best choices for the reinforcement of this elastomer. The clays used in this work—sodium–montmorillonite (Na–Mt) and organically modified versions—were supplied by Southern Clay Products. They were heated for 12 h, at 80 °C under vacuum, to remove residual water.

The Formix Company provided the required mixture of 100 g of natural rubber and the additional ingredients for preparing a commercially cured elastomer (zinc oxide, 3 phr; sulfur,

1.5 phr; stearic acid, 2 phr; cyclohexyl benzothiazole sulfenamide (CBS), 1.5 phr). This material was dissolved in toluene and then mixed with 10 parts per hundred of a given clay with vigorous stirring. The solvent in the resulting dispersion was carefully evaporated and the sample dried under vacuum. The vulcanization was carried out in a standard hot press at 170 °C for 15 min under a pressure adjusted to obtain the required thickness (around 100 microns).

**Characterization.** Small-angle X-ray scattering (SAXS) was used to study the nature and extent of the dispersions of the clays in the filled samples. The SAXS patterns were obtained using a Rigaku diffractometer at the Cu K $\alpha$  wavelength ( $\lambda = 1.54 \text{ \AA}$ ).

Scanning electron micrographs were obtained on a JEOL JSM-5200 model scanning electron microscope.

Ultrathin sections for transmission electron microscopy (TEM) were prepared at –160 °C with a cryo-ultramicrotome (LEICA EM FCS). They had a thickness of  $\approx 60 \text{ nm}$ , and the microscopy was carried out with a Philips CM 120 microscope at a voltage of 80 kV.

Measurements of mechanical properties, birefringence, infrared dichroism, and equilibrium were carried out in the usual manner.

Stress–strain measurements reported here were carried out by simply stretching strips of  $40 \times 10 \times 0.5 \text{ mm}^3$  between two clamps by means of a sequence of increasing weights attached to the lower clamp. The distance between two marks is measured with a cathetometer after allowing sufficient time for equilibration.

To determine the equilibrium swelling of the vulcanizate, a sample of  $20 \times 10 \times 2 \text{ mm}^3$  was put into toluene. After 72 h at room temperature, the sample was taken out of the liquid, the toluene removed from the surface, and the weight determined. The weight swelling ratio,  $Q$ , was also determined from the lengths of the sample in the unswollen and swollen states.

Infrared spectra were recorded with an FTIR spectrometer (Nicolet Model 210) with a resolution of  $4 \text{ cm}^{-1}$  and an accumulation of 32 scans.

Birefringence was measured by using an Olympus BHA polarizing microscope fitted with a Berek compensator.

## Results and Discussion

**Morphology.** SEM micrographs of NR containing 10 wt % of M2 and M3 are shown in Figure 2: the clay particles are dispersed in the elastomeric matrix without much agglomeration of particles. On the basis of those images, the platelet dimensions were on the order of  $1 \mu\text{m}$ .

The microstructures of the rubber composites observed by TEM are shown in Figure 3. Na–Mt dispersed in natural rubber displays typical clay tactoids with layered structures. Obviously, the product obtained was a conventional microcomposite without any intercalation of the clay by the polymer. A different behavior was displayed by the compound with M3. The micrograph

(12) Manna, A. K.; Tripathy, D. K.; De, P. P.; De, S. K.; Chatterjee, M. K.; Pfeiffer, D. G. *J. Appl. Polym. Sci.* **1999**, 72, 1895.

(13) Vu, Y. T.; Mark; J. E.; Pham, L. H.; Engelhardt, M. *J. Appl. Polym. Sci.* **2001**, 82, 1391.

(14) Bala, P.; Samantaray, B. K.; Srivastava, S. K.; Nando, G. B. *J. Mater. Sci. Lett.* **2001**, 20, 563.

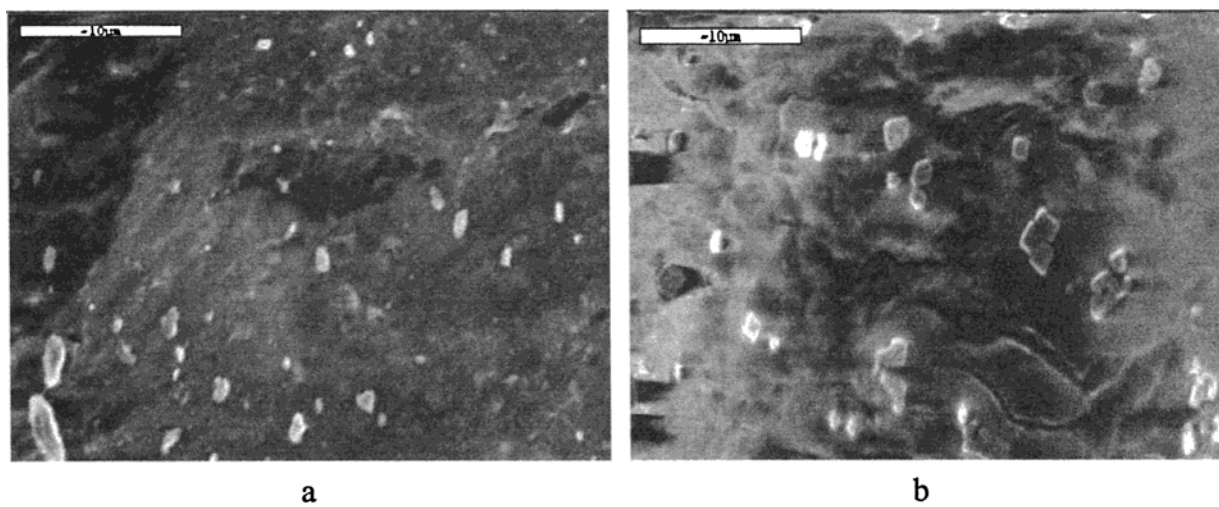


**Figure 2.** SEM micrographs of natural rubber filled with 10 wt % of organoclay: (a) is for M2 and (b) is for M3.



**Figure 3.** TEM micrographs of natural rubber filled with 10 wt % of clay: (a) is for pristine clay (Na-Mt) and (b) is for organo-modified clay (M3). The higher horizontal bar corresponds to 100 nm.

is that of an intercalated system where the clays retain much of their face-to-face alignments, although a small amount does indeed exfoliate.

More direct evidence for the formation of intercalation hybrids is provided by the XRD analysis. As already mentioned, replacing the interlayer cation in the pristine clay with alkylammonium ions enlarges the interlayers from 9.8 Å in Na-Mt to 18.6 and 34.0 Å in M2 and M3, respectively. Further increases of respectively 16.7 and 6.1 Å are observed when the modified clays are dispersed in natural rubber, thus proving the existence of layered clay–polymer intercalates (Figure 4). Vu et al.<sup>13</sup> measured comparable, slightly smaller, interlayer spacing increases of the same organophilic

clays mixed in *cis*-1,4 polyisoprene. Interestingly, in both studies, the increase is much lower with M3 than with M2. This lower extent of swelling of clays modified by bulky ammonium cation has already been reported in the literature. On the other hand, in Figure 4b the scattering ratios  $q_n/q_1$  [where  $q_n = 4\pi n/(\lambda \sin \theta)$  and  $n = 1, \dots, 4$ ] correspond well to the four first permitted reflections in the case of a lamellar diffracting pattern.<sup>15</sup> These harmonics are a strong indication of a very homogeneous swelling of the organo-modified montmorillonite M3, without exfoliation of the lamellae.

(15) Hahn, T. *International Tables for Crystallography*; D. Reidel Publishing Company: Dordrecht, Holland, 1993.

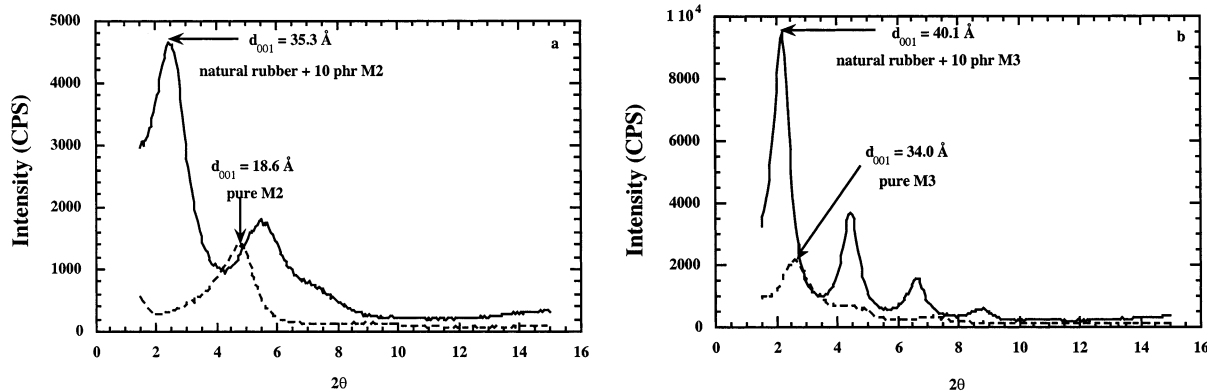


**Figure 4.** X-ray diffraction patterns for pure organo-modified clays and for polymer composites.

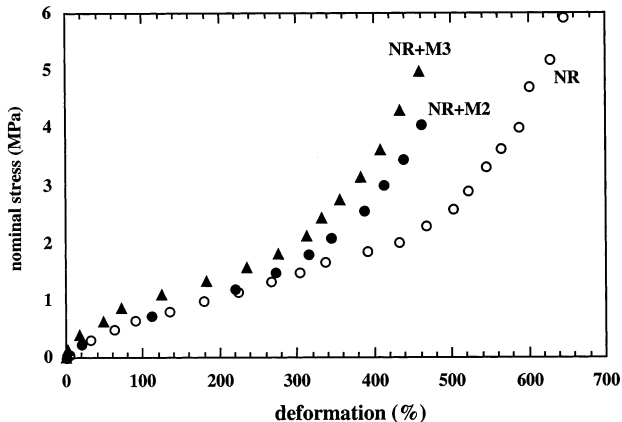


**Figure 5.** Stress-strain curves for natural rubber (NR) and for natural rubber filled with 10 wt % of organically modified clays (M2 and M3).

**Mechanical Properties.** Typical stress-strain curves for the pure natural rubber and the composites containing 10 wt % of modified clay (M2 and M3) are shown in Figure 5. Even at 10 wt %, the modulus increase is comparable to that achieved by higher loadings of conventional micrometer-sized fillers, demonstrating the advantages of a high-surface-area filler.

Other interesting features of elastomeric networks can be revealed by plotting the reduced stress  $\sigma^*$  [ $\sigma^* = \sigma/(\alpha - \alpha^{-2})$ ] against the reciprocal of the extension ratio  $\alpha$  (where  $\sigma$  is the nominal stress defined as the force divided by the undeformed cross-sectional area and  $\alpha$  is the extension ratio, defined as the ratio of the final length of the sample in the direction of stretch to the initial length before deformation) (Figure 6). This representation is suggested by the Mooney–Rivlin equation<sup>16,17</sup>

$$\sigma^* = 2C_1 + 2C_2\alpha^{-1} \quad (1)$$

in which  $2C_1$  and  $2C_2$  are constants independent of  $\alpha$ . An unfilled elastomer that cannot undergo strain-induced crystallization usually displays, at increasing deformations, a decrease in the reduced stress ascribed to the affine–phantom transition.<sup>16</sup> In the case of natural rubber, strain-induced crystallization is observed because of the very uniform microstructure of the polymer chains. It is responsible for the large and

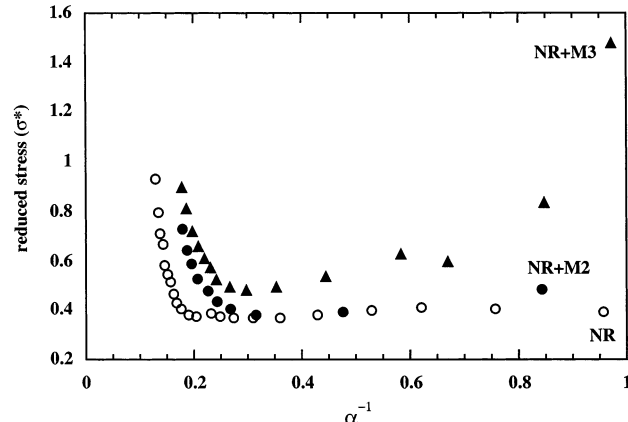


**Figure 6.** Mooney–Rivlin plots for the elastomers.

abrupt increase in the reduced stress observed at deformations approaching the maximum extensibility. This effect corresponds to a self-toughening of the elastomer because the crystallites act as additional cross-links in the network, strain amplifiers, and to some extent as filler particles. When compounded with a reinforcing filler, elastomers do exhibit upturns in the modulus attributed to the limited chain extensibility of short chains bridging neighboring filler particles.<sup>18,19</sup> The upturn in the modulus is observed if a strong interaction between polymer and filler exists. The results displayed in Figure 6 show that natural rubber filled with modified clays obviously exhibits upturns in the modulus at smaller deformations than that observed in a pure elastomer. In this case, the upturns in the moduli are most likely associated with the strain-induced crystallization. One would expect the intercalated polymer chains to be in a more extended conformation than those outside the clay galleries, thus favoring the crystallization process. A characteristic feature observed in the infrared of pure natural rubber upon crystallization is the shift of the C–H out-of-plane frequency from 837 to 841  $\text{cm}^{-1}$  (Figure 7a). The 841- $\text{cm}^{-1}$  absorption band can be considered to be specific to crystalline material.<sup>20,21</sup> The same effect is observed in the presence of clay (Figure 7b).

On the other hand, a large decrease in the modulus is obtained for the compound with M3 attributed to the

(16) Mark, J. E.; Erman, B. *Rubber Elasticity. A Molecular Primer*; Wiley-Interscience: New York, 1988.

(17) Erman, B.; Mark, J. E. *Structures and Properties of Rubberlike Networks*; Oxford University Press: New York, 1997.

(18) Bokobza, L. *Polymer* **2001**, *42*, 5415.

(19) Bokobza, L. *Macromol. Symp.* **2001**, *169*, 243.

(20) Gotoh, R.; Takenaka, T.; Hayama, N. *Kolloid Z. Z. Polym.* **1965**, *20*, 18.

(21) Amram, B.; Bokobza, L.; Queslet, J. P.; Monnerie, L. *Polymer* **1986**, *27*, 877.

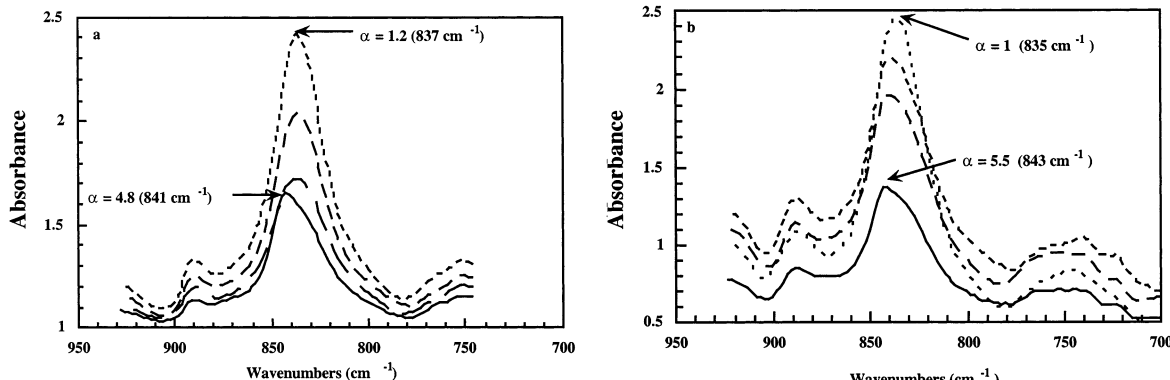


**Figure 7.** Shift of the out-of-plane absorption band upon stress-induced crystallization: (a) is for pure natural rubber and (b) is for natural rubber filled with M2.

Payne effect. This effect originates from the destruction of filler networking formed by filler–filler interactions in the case of a highly polar filler such as silica, or via immobilized layers on the filler surface in the case of strong interactions between filler and rubber. The Payne effect, usually evidenced through the analysis of the low-strain dynamic properties, is characterized by a strong decrease in the storage modulus  $G'$ , associated with a maximum of the loss modulus  $G''$  and of  $\tan \delta$  ( $\text{tg}\delta$ ).<sup>22–24</sup> In the previous study cited,<sup>13</sup>  $\text{tg}\delta$  of the compounds with M3 was found to be larger than that with M2. In the case of conventional particulates, the increase in the modulus imparted by an active filler is reasonably well understood. It involves a hydrodynamic effect arising from the inclusion of rigid particles and an increase in the cross-link density created by polymer–filler bonding.

The inclusion of rigid filler particles is quantitatively taken into account by the Guth and Gold equation<sup>25,26</sup> given by

$$G = G_0(1 + 2.5\varphi + 14.1\varphi^2) = G_0X \quad (2)$$

where  $G_0$  is the modulus of the matrix and  $\varphi$  is the volume fraction of the filler. This equation is based on the Einstein's equation for the viscosity of a suspension of spherical rigid particles.<sup>27</sup>

Guth and Gold generalized the Einstein concept by adding the quadratic term to account for interaction between particles. For nonspherical particles, a shape factor  $f$ , defined as the ratio of particle length to width, was introduced:

$$G = G_0(1 + 2.5\varphi f + 14.1\varphi^2 f^2) \quad (3)$$

Since the anisotropic character is important in layered silicates, a shape factor has to be taken into account in predicting a clay-reinforced nanocomposite modulus, with an effective volume fraction larger than the theoretical one.

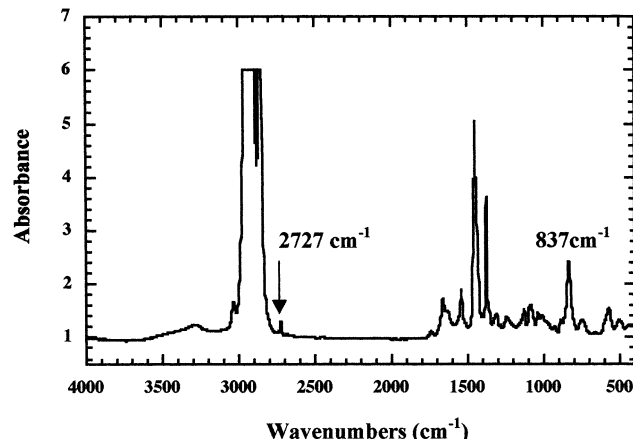


**Figure 8.** Mid-infrared spectrum of natural rubber.

In conventionally filled polymers, a second contribution to the modulus arises from filler–rubber interactions, leading to an introduction of additional cross-links into the network by the filler and increasing the effective degree of cross-linking. In clay composites, besides the confinement of polymer chains between the silicate layers, there could also be interactions of polymer chains with the long alkyl groups of the organically modified clays. Measurements of chain orientation and swelling experiments have been shown to provide a direct estimation of the total network chain density arising from chemical junctions and also from the density of polymer–filler attachments.<sup>18,19</sup> On the other hand, it is relevant to compare the total degree of polymerization to that of the unfilled network to check whether the intragallery polymerization is hindered.

**Evaluation of the Total Network Density.** Chain orientation under uniaxial extension is only sensitive to the total cross-link density, as opposed to the stress–strain measurements which contain contributions from the inclusion of rigid particles. It can be evaluated either by birefringence or by infrared dichroism techniques, two techniques widely described elsewhere.<sup>18,28</sup>

The infrared dichroism technique is based on the measurement of the orientation of a specific transition moment vector associated with a vibrational mode. The anisotropy consecutive to the applied deformation is characterized by the dichroic ratio  $R$  of a selected absorption band defined as  $R = A_{\parallel}/A_{\perp}$ . Here,  $A_{\parallel}$  and  $A_{\perp}$

(22) Payne, A. R. *J. Polym. Sci.* **1962**, *6*, 57.

(23) Payne, A. R.; Whittaker, R. E. *Rubber Chem. Technol.* **1971**, *44*, 440.

(24) Payne, A. R. In *Reinforcement of Elastomers*; Kraus, G., Ed.; Interscience Publishers: New York, 1965; Chapter 3.

(25) Guth E.; Gold, O. *Phys. Rev.* **1938**, *53*, 322.

(26) Guth, E. *J. Appl. Phys.* **1945**, *16*, 20.

(27) Einstein, A. *Ann. Phys. (Leipzig)* **1906**, *19*, 289.

(28) Bokobza, L. *Polym. Int.* **2000**, *49*, 743.

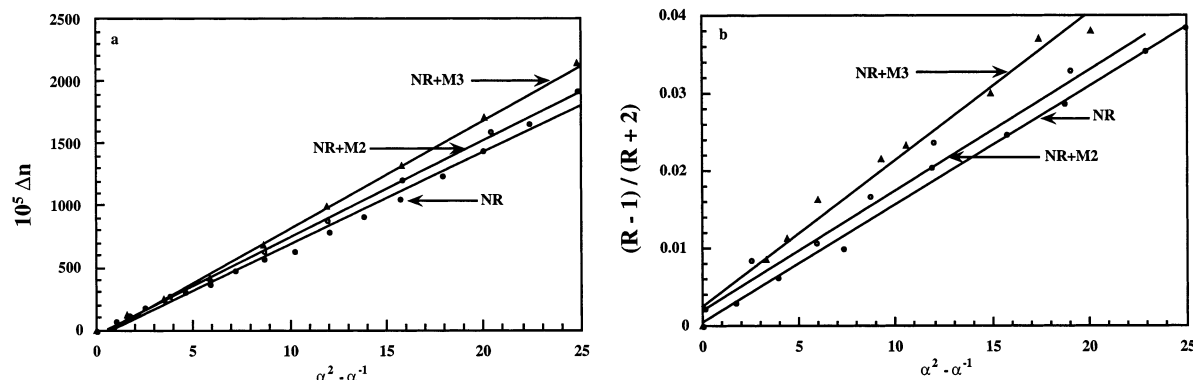


**Figure 9.** Orientation of polymer chains: (a) is for birefringence and (b) is for infrared dichroism.

are the absorbances of the investigated band measured with radiation polarized parallel and perpendicular to the stretching direction, respectively.<sup>28–31</sup> The orientation of the transition moment vector with respect to the direction of stretch is expressed in terms of the second Legendre polynomial  $\langle P_2(\cos \gamma) \rangle$  related to the dichroic ratio by

$$\langle P_2(\cos \gamma) \rangle = \frac{R - 1}{R + 2} \quad (4)$$

The orientation function  $\langle P_2(\cos \gamma) \rangle$  which characterizes the orientation of the transition moment vector relative to the direction of stretch in uniaxially deformed networks is obtained, for an affine network, from

$$\langle P_2(\cos \gamma) \rangle = D_0(\alpha^2 - \alpha^{-1}) \quad (5)$$

where  $D_0$  is the configurational factor defined by<sup>30</sup>

$$D_0 = (3\langle r^2 \cos^2 \Phi \rangle_0 / \langle r_2 \rangle_0 - 1) / 10 \quad (6)$$

Here,  $\Phi$  is the angle between the transition moment vector whose orientation is being considered and the chain end-to-end vector  $r$ . The averaging is performed for unconstrained chains. The moments  $\langle r^2 \rangle_0$  and  $\langle r^2 \cos^2 \Phi \rangle_0$  in eq 7 can be calculated by the matrix generation technique of the rotational isomeric state formalism. The configurational factor  $D_0$ , which incorporates the structural features of the network chains, is inversely proportional to the number  $n$  of bonds in the chain between two junctions.<sup>30</sup>

In the case of affine behavior, the birefringence is related to the strain function by the expression<sup>33,34</sup>

$$\Delta n = \frac{\nu k T C}{V} (\alpha^2 - \alpha^{-1}) = D_1(\alpha^2 - \alpha^{-1}) \quad (7)$$

where  $\nu/V$  represents the number of chains per unit volume.  $C$  is the stress-optical coefficient defined as  $C = \Delta n/\sigma_t$ , where  $\sigma_t$  is the true stress (force  $f$  divided by

(29) Amram, B.; Bokobza, L.; Monnerie, L.; Queslet, J. P. *Polymer* **1988**, *29*, 1155.

(30) Bokobza, L.; Amram, B.; Monnerie, L. *Elastomeric Polymer Networks*; Mark J. E., Erman, B., Eds.; Prentice Hall: Englewood Cliffs, NJ, 1992; p 28.

(31) Bokobza L.; Macrom, C. *The Wiley Polymer Networks Group Series Vol. 2*; Stokke B. T., Elgsaeter, A., Eds.; John Wiley and Sons: New York, 1999; p. 199.

(32) Besbes, S.; Cermelli, I.; Bokobza, L.; Monnerie, L.; Bahar, I.; Erman, B.; Herz, J. *Macromolecules* **1992**, *25*, 1949.

(33) Erman, B.; Flory, P. J. *Macromolecules* **1983**, *16*, 1601.

(34) Erman, B.; Flory, P. J. *Macromolecules* **1983**, *16*, 1607.

the deformed area). The slopes of the strain dependences of the orientation function  $D_0$  and of the birefringence  $D_1$  vary as  $1/M_c$  (where  $M_c$  is the molecular weight between cross-links). Both measurements are thus suitable for an evaluation of the effective cross-link density arising from the chemical junctions and also from the polymer–filler interactions.

The mid-infrared spectrum of the unfilled network is represented in Figure 8.

Because of the strong intensity of the bands associated with the fundamental modes, we have examined the dichroic behavior of the band located at  $2727 \text{ cm}^{-1}$ .

Figure 9 shows the strain dependence of the birefringence and that of the dichroic function  $(R - 1)/(R + 2)$  for the unfilled natural rubber and for the two composites. An increase in the orientational level of polymer chains, evidenced by birefringence and by infrared dichroism, is observed upon incorporation of the clay. An increase in orientation, observed in the case of active conventional fillers, has been associated with an increase in the cross-link density attributed to filler–rubber interactions, leading to an introduction of additional cross-links into the network by the filler.<sup>18,19</sup> The interaction between clay and natural rubber can predominantly occur via the alkyl chains of the ammonium cation and could arise from van der Waals forces or through entanglements. Most probably, the clay particles tend to orient along the direction of the applied force and the adsorption of polymer segments at several sites of the filler particle introduces further cross-linking into the system, which increases the network chain density. Recently, a high degree of orientation of the silicate layers under uniaxial deformation was evidenced in rubber compounds based on butadiene rubber or styrene–butadiene rubber containing organophilic silicates.<sup>35</sup> The authors focused on the orientation of the silicate layers, monitored by means of online WAXS measurements. In the present study, attention has been paid only to the orientation of the polymer chains in the presence of the clay particles. Further investigations will be carried out to investigate the orientation of the clay particles themselves by looking at specific absorption bands of the filler. This would give insight into the mechanism of reinforcement provided by highly anisotropic fillers and accounted for in the shape factor appearing in eq 3.

(35) Ganter, M.; Gronski, W.; Reichert, P.; Mülhaupt, R. *Rubber Chem. Technol.* **2001**, *74*, 221.

The degree of swelling of a network at equilibrium depends on several factors including the lengths of the network chains. The average molecular weight  $M_c$  between cross-links can be estimated from the equilibrium swelling ratio  $Q = V/V_0$ , where  $V$  is the volume of the network plus solvent and  $V_0$  is the volume of the dry network.<sup>16,17</sup> This swelling procedure was applied to the filled vulcanizates to evaluate the number of filler–rubber attachments. Under the assumption that the filler particles do not swell at all, one can calculate the equilibrium swelling ratio of the rubber phase  $Q_r$  from the equilibrium swelling ratio  $Q$  of the composite and from the filler fraction  $\phi$ :

$$Q_r = (Q - \phi)/(1 - \phi) \quad (8)$$

The rubber swelling ratio was found to be equal to 4.93 for natural rubber swollen in toluene, but when the polymer is compounded with M2 and M3, it decreases to 4.67 and 4.56, respectively. This restricted swelling of the rubber by the organo-clay would reflect a small increase in the effective cross-link density.

## Conclusions

Organically modified galleries of montmorillonites are easily penetrated by natural rubber chains and lead to intercalated structures and partial exfoliation. Large increases in modulus are observed even at rather low filler loadings. The increase in the modulus is most probably associated with the inclusion of solid particles exhibiting a high anisotropy of the layers. Nevertheless, as the mechanisms of reinforcement by highly anisotropic fillers are not understood at the present time, further investigations are required to know if the basic processes contributing to the stress–strain behavior of vulcanizates filled with conventional fillers are also valid for these more complex systems.

**Acknowledgment.** It is a pleasure to acknowledge the financial support provided to J.E.M. by the National Science Foundation through Grant DMR-0075198 (Polymers Program, Division of Materials Research).

CM020093E